Uzbek Journal of Physics
DOI: https//doi.org/10.52304/.v27i1.598

Noncoincidence effect in the C-O and O-H stretching modes of methanol: a polarized Raman and DFT study

A. Jumabaev[*,1], H.A. Hushvaktov[1], U.A. Holikulov[1], Sh.Sh. Yormatov[1], B.E. Niyazkhanova[2]

[1] Samarkand State University, University blv.15, 140104, Samarkand, Uzbekistan
[2] Bukhara State University, M. Ikbol str. 11, 200118, Bukhara, Uzbekistan

Received 21.01.2025, revised 03.03.2025

* Corresponding author: e-mail:, jumabaev2@rambler.ru Tel. +998 93 722 52 65

В этом исследовании оптимальная геометрия и колебательные свойства метанола анализируются с помощью теория функционала плотности (ТФП) и поляризованной рамановской спектроскопии. Структура глобального минимума молекулярных кластеров метанола получена с использованием программного обеспечения ABCluster. ТФП и пограничная молекулярная орбиталь (ПМО) использованы для структурного и термодинамического исследования различных молекулярных кластеров метанола. С помощью этих методов рассчитаны потенциальные энергии межмолекулярного взаимодействия и энергии щели HOMO-LUMO димерных, тримерных и тетрамерных кластеров метанола. В результате идентифицированы димер-спиральные, циклические тримерудовые и циклические тетрамерудовые кластеры с наибольшей структурной и термодинамической стабильностью метанола. Экспериментальными и расчетными методами определены изотропные и анизотропные компоненты спектральных полос метанола С-О и О-Н. Полученные данные показали, что в димерном кластере не может образоваться анизотропная компонента. Установлено, что характеристики поляризованного спектра комбинационного рассеяния циклического тетрамерного кластера аналогичны экспериментальным результатам.

Ключевые слова: ТФП, ПМО, изотропия, анизотропия, эффект рамановского несовпадения.

In this study, the optimal geometry and vibrational properties of methanol were analysed by the density functional theory (DFT) approach and polarized Raman spectroscopy. Global minimum structures of methanol molecular clusters were generated using ABCluster software. DFT and frontier molecular orbital (FMO) were applied to structurally and thermodynamically investigate various methanol molecular clusters. Using these methods, the intermolecular interaction potential energies and HOMO-LUMO gap energies of methanol dimer, trimer, and tetramer clusters were calculated. As a result, dimer-helical, cyclic trimer-uud, and cyclic tetramer-udud clusters with the highest structural and thermodynamic stability of methanol were identified. Experimental and computational methods were used to determine the isotropic and anisotropic components of the methanol C-O and O-H spectral bands. The data obtained showed that an anisotropic component cannot form in the dimer cluster. The characteristics of the polarized Raman spectrum of the cyclic tetramer cluster were found to be similar to the experimental results.

Keywords: DFT, FMO, isotropic, anisotropic, Raman noncoincidence effect.

t

I. Introduction

In the late twentieth century, there was an increase of interest in exploring intermolecular interactions and molecular orientation in liquids [1, 2, 3]. Molecular characteristics are investigated using a variety of experimental and theoretical methods. Polarized Raman spectroscopy is one of these experimental methods. This method can determine the isotropic and

anisotropic components of Raman scattered light [5]. Many studies show that the wave numbers of these components differ from each other. This phenomenon is known as the noncoincidence effect (NCE). P. Mirone [1], J.L. McHale [2, 3, 4] and D.E. Logan [6, 7] analyzed NCE in polar and nonpolar liquids using theoretical methods. They created a dielectric continuum model to explain the NCE phenomenon. H. Torii et al. [8] suggested that the NCE depends on a transition dipole-transition dipole interaction between adjacent molecules. Transition dipole-transition dipole interaction refers to the coupling between the transition dipole moments of neighboring molecules or molecular groups during electronic or vibrational transitions. Also [9], they additionally carried out molecular (MD) dynamics simulations to investigate NCE in liquids. Knapp [10] explained that the reason for this phenomenon is resonance energy transfer. NCE was observed experimentally by T.W. Zerda and his scientific team [11]. They showed that the difference between the anisotropic and isotropic components of the C-O spectral band of methanol is $\Delta\nu = -5$ cm^{-1}. The NCE of the carbonyl stretching band of methyl formate ($HCOOCH_3$) diluted in acetonitrile was investigated by R.J. Bartholomew and D.E. Irish [12]. They analyzed the carbonyl bandwidths and observed that they first increased and then decreased. A. Sokolowska [13] studied methanol solutions in carbon tetrachloride and concluded that NCE is caused by a mismatch in local molecular order. M.G. Giorgini et al. [14, 15, 16] used experimental, theoretical, and Monte Carlo (MC) simulation methods to analyze the NCE of liquids in various solvents. They concluded that these methods support each other in explaining NCE in liquids. Musso et al. [17] investigated the NCE of C-O and O-H vibrational bands in methanol/CCl_4 solutions and its dependence on concentration using Raman spectroscopy and molecular dynamic (MD) simulations. They stated that MD models could not explain the sharp decrease in the ν(C-O) band when methanol was diluted to a fraction of $X_m < 0.1$ in CCl_4. G. Döge at al. [18] experimentally determined the negative NCE in aromatic ring vibrations. They also investigated the NCE in aliphatic ring vibrations. G. Devi et al. [19] studied the role of repulsive force on the effect of anisotropic shift in liquids. In addition, they experimentally determined the effect of various solvents on the S=O vibrational mode of DMSO and compared it with four theoretical models, such as McHale's, Mirone's modification of McHale's, Logan's, and Onsager-Fröhlich dielectric continuum models, respectively [20]. D.K. Singh et al. [21] analyzed the solution of methanol and ethanol in acetonitrile. They applied polarized Raman spectra and quantum chemical calculations to investigate how the spectrum depends on molecular structure. F.H. Tukhvatullin et al. [22, 23] investigated the structure of a methanol-aqueous solution using Raman spectroscopy and ab initio calculation methods. They found that the formation of intermolecular hydrogen bonds, as well as O-H or O-D vibrations in pure alcohol, complicates Raman spectra, resulting in a noncoincidence of the peak frequencies, a shift of the band to the low-frequency region, and a strong broadening of the bond halfwidth. Q. Shi et al. [24] studied the NCE of C-O stretching of methanol in aqueous solution by theoretical Raman spectroscopy. They observed a slight increase in the NCE from $X_m = 0.4$ to $X_m = 0.3$ and attributed this to the band asymmetry caused by the reorientation dynamics. Since molecular orientation plays an important role in the study of the structural properties of liquids and crystals, the study of the NCE is currently the focus of attention of scientists in this field. Nowadays, in addition to polarized Raman spectroscopy, aggregation-induced split (AIS) theory and HNMR are used to study this phenomenon [25, 26, 27].

In this paper, the NCE in the C-O and O-H vibrational bands of methanol is discussed using polarized Raman spectroscopy and density functional theory (DFT) methods.

II. Experimental and computational details

The polarized Raman spectra of pure methanol were recorded using a Renishaw InVia Raman spectrometer at room temperature. As a source of excitation light, an argon laser with a wavelength of 532 nm, a power of 50 mW, and a diffraction grating with a period of 1200 lines/mm was used. The scarred light was recorded using a standard Renishaw CCD Camera detector. Polarized Raman spectroscopy is based on the determination of parallel ($I_{||}$) and perpendicular ($I_{\perp}$) components of scattered light. According to [28]:

$$I_{||} = A(\nu_0 - \nu)^4 \left((45\alpha^2 + 4\gamma^2) / 45 \right) Q^2, \quad (1)$$

$$I_{\perp} = A(\nu_0 - \nu)^4 \left(2\gamma^2 / 15 \right) Q^2, \quad (2)$$

where α – rotational invariant isotropy and γ – anisotropy of transition polarizability. Using these components, it is possible to determine the isotropic and anisotropic components of the Raman spectrum: $I_{isot} = I_{||} - 4/3I_{\perp}$, $I_{anisot} = I_{\perp}$.

According to (1) and (2), depolarization ratio of Raman line:

$$\rho = I_{\perp} / I_{\parallel} = 3\gamma^2 / (45\alpha^2 + 4\gamma^2) \quad (3)$$

According to (3):

– for totally symmetric vibrations ρ = 0,

– for partial symmetric vibrations 0 < ρ < 0.75,

– for totally asymmetric vibrations ρ = 0.75.

The isotropic and anisotropic wave numbers of the vibration spectrum are found as follows [9]:

$$\nu_{isot} = \sum_{i=1}^{n} I_i^{isot} \nu_i / \sum_{i=1}^{n} I_i^{isot}, \quad (4)$$

$$\nu_{isot} = \sum_{i=1}^{n} I_i^{anisot} \nu_i / \sum_{i=1}^{n} I_i^{anisot}, \quad (5)$$

where ν_i is the wave number of each streching mode, I_i^{isot} and I_i^{anisot} are the Raman intensities corresponding to each isotropic and anisotropic stretching frequency.

Density functional theory (DFT) method with B3LYP/6–311++G (*d*, *p*) function set was used to optimize methanol molecule and its clusters. For identifying the most stable clusters, we used the artificial bee colony (This is an extension of the program ABC). ABC algorithm implemented by the ABCluster software [29] with DFT. All computations were performed using the Gaussian 09W program package [30]. Gaussview 6.0 [31] tool was used to visualize the results. Intermolecular interaction energies Δ*E* in clusters are calculated by following formula [32]:

$$\Delta E = E_{cluster} - nE_{monomer}, \quad (6)$$

where *n* – number of molecules in methanol clusters, $E_{monomer}$ and $E_{cluster}$ are total energies of methanol monomer and clusters, respectivily.

III. Results and discussion

III.1. Experimental studies

In this work, we studied the polarized Raman spectra of the C-O and O-H spectral bands of methanol. Figure 1 shows the isotropic and anisotropic components of the Raman spectrum of pure liquid methanol in the range of 950–1100 cm^{-1}.

The maxima of the isotropic and anisotropic components of the spectral bands of *ν*(C-O) are located at 1035 and 1030 cm^{-1}, respectively. From these data, the NCE value of the C-O spectral band is –5 cm^{-1}. This value is the same as the result obtained by other researchers [11]. Figure 2 shows the isotropic and anisotropic components of the Raman spectrum of pure methanol in the range of 3100–3700 cm^{-1}. It can be seen from the figure that both spectral bands have high asymmetry. Therefore, the wave numbers of these bands were determined from formulas (4) and (5). Hence, the isotropic and anisotropic wavenumbers of the *ν*(O-H) bands are 3350 and 3425 cm^{-1}, respectively. From these data, the NCE value of the O-H spectral band is +75 cm^{-1}. This result is exactly the same as the results obtained by other researchers [5]. According to H. Torii [8], the formation of the NCE is a transition dipole-transition dipole interaction between neighboring molecules. The obtained results showed that different NCEs are formed in two different types of vibrational bands of methanol molecules. That is, both positive and negative NCEs occur.

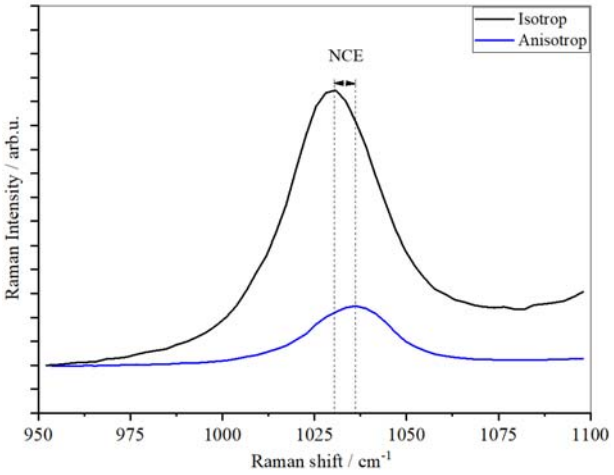

Figure 1. Isotropic and anisotropic components of *ν*(C-O) stretching Raman bands of liquid methanol.

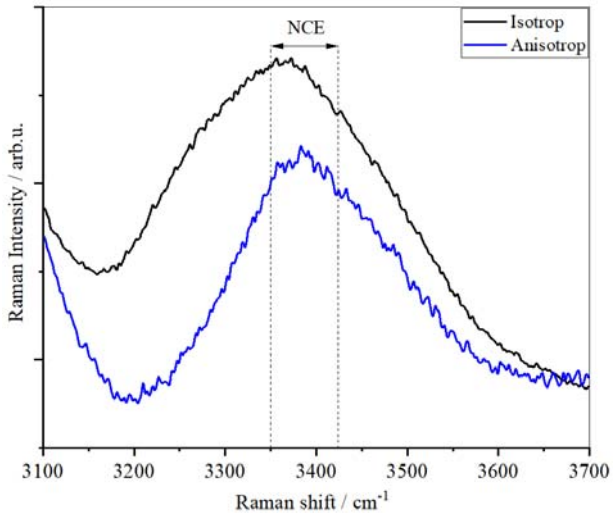

Figure 2. Isotropic and anisotropic components of *ν*(O-H) stretching Raman bands of liquid methanol.

III.2. Computational studies

To better explain this phenomenon, we analyzed self-association clusters of methanol in DFT. Initially, we tried to identify the most stable methanol clusters in order to analyze the pair dipole-dipole orientation and calculate Raman spectra. Different structures of methanol clusters have been investigated before using different studies. For example, R. Ludwig [33] and S.L. Boyd [34] showed in their scientific works that cyclic clusters of methanol are more stable than other types of clusters. The difference between this work and previous works is that the global minimum structures of methanol clusters were generated using ABCluster. Today, this program is an innovative method for determining the optimal geometry of various molecular clusters [35, 36]. Figure 3 shows the optimal geometric structures of dimers, cyclic trimers and tetramers calculated at the B3LYP/6–311++G (*d*, *p*) level using the DFT method. Intermolecular interaction energies in molecular clusters are 7.5 kcal/mol for the helical-structure dimer (Fig. 3a) and 0.17 kcal/mol for the stacked-structure dimer (Fig. 3b), respectively. By comparing the intermolecular interaction energies, it can be seen that the helical-dimer is more stable than the stacked-dimer ($\Delta E_{\text{helical-dimer}} >> \Delta E_{\text{stacked-dimer}}$). Intermolecular interaction energies in molecular clusters are 10 kcal/mol for the uud-trimer and 8.5 kcal/mol for the planar-trimer. According to $\Delta E_{\text{uud-trimer}} > \Delta E_{\text{planar-trimer}}$, uud-trimer is more stable than planar-trimer. Also, intermolecular interaction energies in molecular clusters are 19.88, 19.57, 19.54 and 19.2 kcal/mol for the udud-tetramer, (up-down-up-down) uudd-tetramer, (up-up-down-down) uuud-tetramer and uuuu-tetramer, respectively (these are designations for the orientation of the CH_3 groups in the methanol tetramer relative to the cyclic plane). The results show intermolecular interaction energies in tetramers in order to $\Delta E_{\text{udud-tetramer}} > \Delta E_{\text{uudd-tetramer}} > \Delta E_{\text{uuud-tetramer}} > \Delta E_{\text{uuuu-tetramer}}$ and the udud-tetramer is more stable than other tetramers. The calculated results confirm that clusters helical-dimer, uud-trimer, and udud-tetramer are more stable according to of intermolecular interaction energy.

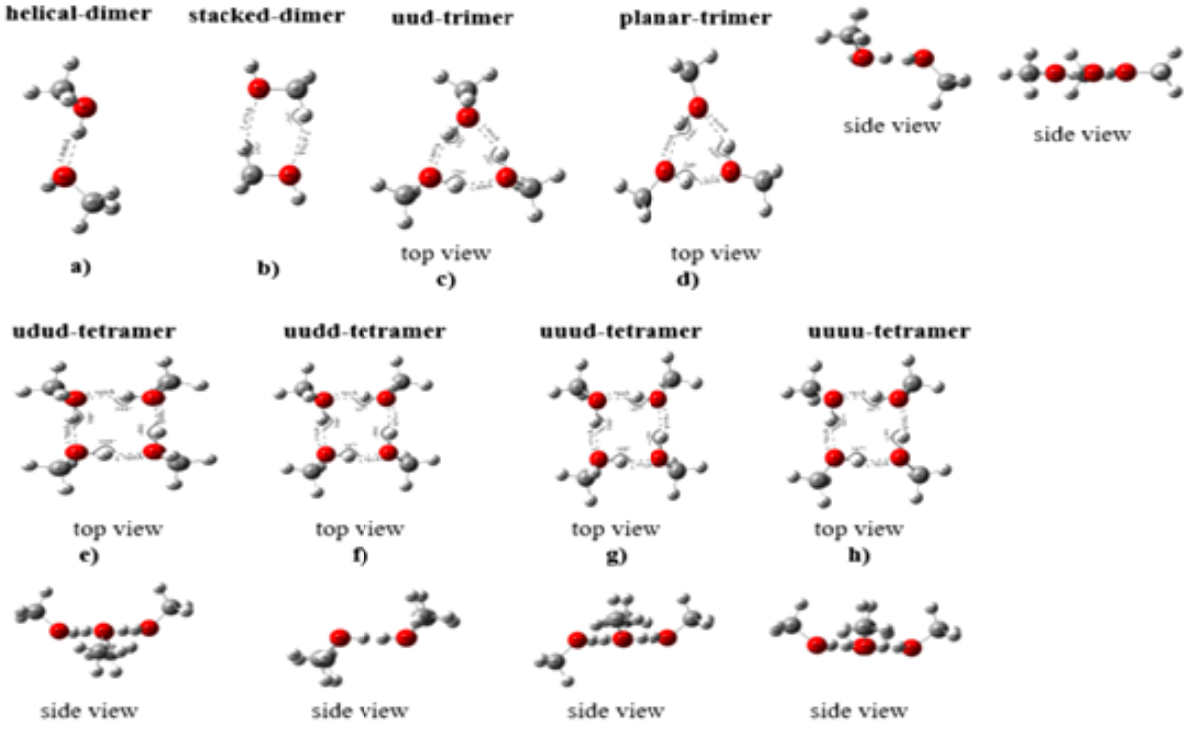

Figure 3. Optimized structures of methanol clusters: **a**, **b** – dimers, **c**, **d** – trimers (top and side view) and **e-h** – tetramers (top and side view).

Dipole-dipole orientation. We didn't investigate the dipole-dipole orientation in the dimer since the molecules can't form a closed cluster. As a result, the molecular orientation causes the dipole-dipole inte raction to be zero. Figure 4(a) shows a pair of mutually parallel C-O bonds connected by hydrogen bonds

in the trimer cluster. The length and angle of the hydrogen bond formed between them are 1.906 Å and 150°, respectively. The distance between C-O bonds is 3.698 Å. The angles formed by these bonds with respect to the axis connecting their centers are 125° and 134°, respectively. Similarly, Figure 4(b) shows a parallel C-O pair connected by hydrogen bonds in the tetramer cluster. The length and angle of the hydrogen bond formed between them are 1.769 Å and 167°, respectively. The distance between the centers of C-O bonds is 4.866 Å. The angles formed by these bonds with respect to the axis connecting their centers are 134° and 134°, respectively.

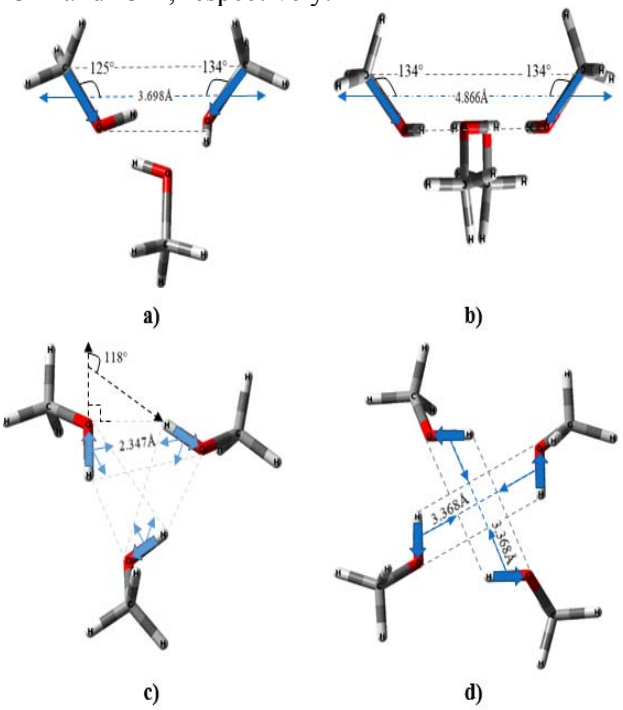

Figure 4. Isotropic and anisotropic components of *v*(O-H) stretching Raman bands of liquid methanol.

Figure 4(c) shows a pair of mutually antiparallel O-H bonds connected by hydrogen bonds in the trimer cluster. The length and angle of the hydrogen bond formed between them are 1.906 Å and 150°, respectively. The distance between the centers of O-H bonds is 2.347 Å. The angles formed by these bonds with respect to the axis connecting their centers are 90° and 30°, respectively. Also, Figure 4(d) depicts the antiparallel O-H pair of the tetramer. The length and angle of the hydrogen bond formed between them are 1.769 Å and 167°, respectively. The distance between the centers of C-O bonds is 3.368 Å. The figure shows that the tetramer's O-H bond pairs are totally antiparallel-oriented. From these results, we can conclude that the parallel C-O and O-H bonds in the tetramer form stronger hydrogen bonds than the same pairs in the trimer. In addition, the C-O and O-H pairs in the tetramer have a very high-order symmetric orientation, and the pairs in the trimer have an asymmetric orientation. As a result, the tetramer has a stronger dipole-dipole interaction than the trimer.

Frontier molecular orbital (FMO) analysis. FMO analysis was performed to confirm which molecular cluster was more thermodynamically stable. The highest occupied molecular orbital (HOMO) and the lowest unoccupied molecular orbital (LUMO) are known as frontier molecular orbitals (FMO), and their values can be used to analyze intermolecular interactions and the electron donating and accepting abilities of molecules [37, 38]. The energy gap (E_g) accurately predicts the molecules kinetic and thermodynamically stability [39].

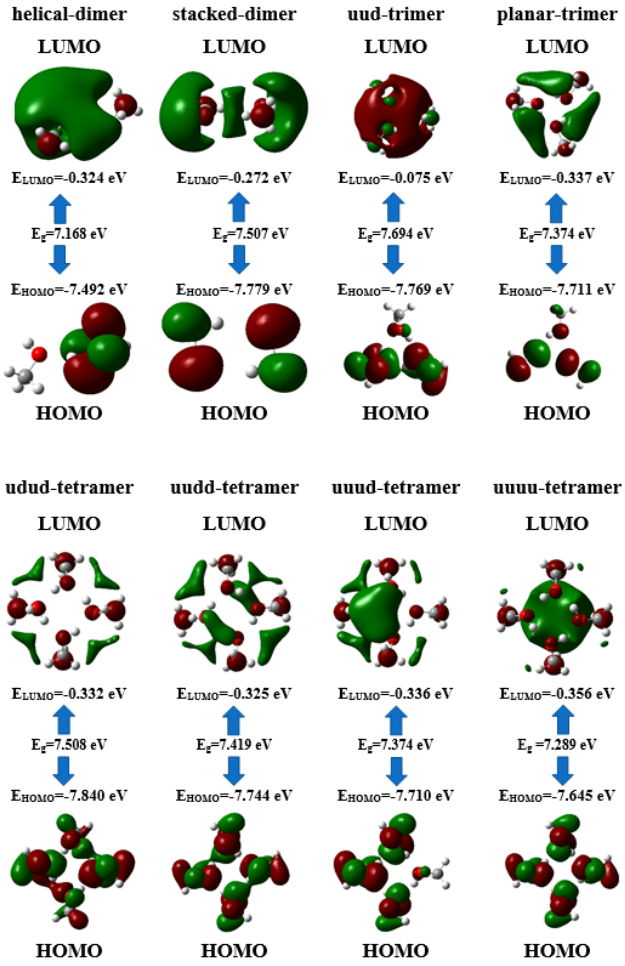

Figure 5. HOMO-LUMO maps of methanol clusters.

Figure 5 indicates the HOMO and LUMO orbitals of the methanol clusters. These values are determined using the following mathematical formulas based on Koopman's theorem [40]:

$$E_g = E_{\mathrm{HOMO}} - E_{\mathrm{LUMO}}, \quad (7)$$

$$\eta = (E_{\mathrm{HOMO}} - E_{\mathrm{LUMO}})/2, \quad (8)$$

where the chemical reactivity parameters: – energy gap and – hardness.

According to [41], the larger the , the harder (or more stable) the system, and *vice versa*. The calculated HOMO energy values of uud-trimer and planar-trimer are −0.075 eV and −0.337 eV, respectively. The calculated LUMO energy values of uud-trimer and planar-trimer are −7.769 and −7.711 eV, respectively. The calculated HOMO energy values of udud-tetramer, uudd-tetramer, uuud-tetramer and uuuu-tetramer are −0.332, −0.325, 0.336 and 0.356 eV, respectively. The calculated LUMO energy values of udud-tetramer, uudd-tetramer, uuud-tetramer and uuuu-tetramer are −7.840, −7.744, 7.710 and 7.645 eV, respectively. According to the formula (7), the relationship between the HOMO-LUMO energy gaps of uud-trimer and planar-trimer is E_{uud} (7.694 eV)> E_{planar}(7.374 eV). Similarly, the relationship between the HOMO-LUMO gap energies of tetramer clusters is E_{udud} (7.503 eV)>E_{uudd}(7.419 eV)>E_{uuud}(7.374 eV)> E_{uuuu}(7.289 eV). We neglected dimer$_{\mathrm{helical}}$ and dimer$_{\mathrm{s\text{-}tacked's}}$ HOMO-LUMO gap energy because their intermolecular interaction energies differed significantly. Considering the formula (8), then $\eta_{\mathrm{uud}}>\eta_{\mathrm{planar}}$ and $\eta_{\mathrm{udud}}>\eta_{\mathrm{uudd}}>\eta_{\mathrm{uuud}}>\eta_{\mathrm{uuuu}}$ for trimers and tetramers, respectively. The FMO analysis confirms that the uud-trimer and udud-tetramer are more stable than other similar clusters. Using all of the above confirmations, we analysed the calculated Raman spectra of helical-dimer, uud-trimer, and udud-tetramer.

III.3. Theoretically calculated vibrational analysis

C-O stretching. Figure 6 shows the calculated Raman spectra of the C-O stretching vibrational bands of the most stable methanol clusters. The wave number of C-O (ρ=0.28, isotropic) stretching of methanol monomer is 1038 cm^{-1} (in the experiment 1035 cm^{-1}). The calculated Raman spectra show that wave number of *v*(C-O) involved in H-bonding in the dimer is 1017 cm^{-1} and depolarization ratio is 0.27. In contrast, the vibrational wave number not involved in H-bonding is 1040 cm^{-1}. Its depolarization ratio is 0.28, where both components are isotropic. Because the dimer is not cyclic (or not closed), the molecules within it can rotate freely. This causes the potential energy of the dipole-dipole interaction to become zero, because the dipole-dipole interaction is highly dependent on the molecular orientation. The spectrum of the trimer was observed, in addition to the isotropic component, an anisotropic component formed. In this case, the wave number and depolarization ratio of the isotropic component are 1042 cm^{-1} and 0.09, respectively. The wave number and depolarization ratio of the anisotropic component are 1030 cm^{-1} and 0.75, respectively. The difference in wave number between these components:
1030–1042=–12 cm^{-1} Similarly, an anisotropic component was observed in the tetramer spectrum. The wave number of isotropic component is 1044 cm^{-1} and its depolarization ratio is 0. As well as the wave number of anisotropic component 1036 cm^{-1} and its depolarization ratio is 0.75. The NCE for tetramer: 1036–1044=–8 cm^{-1} (the experimental value is –5 cm^{-1}). The calculated Raman spectra of the C-O spectral bands showed that the value of NCE in the tetramer is closer to the experimental value than in the trimer.

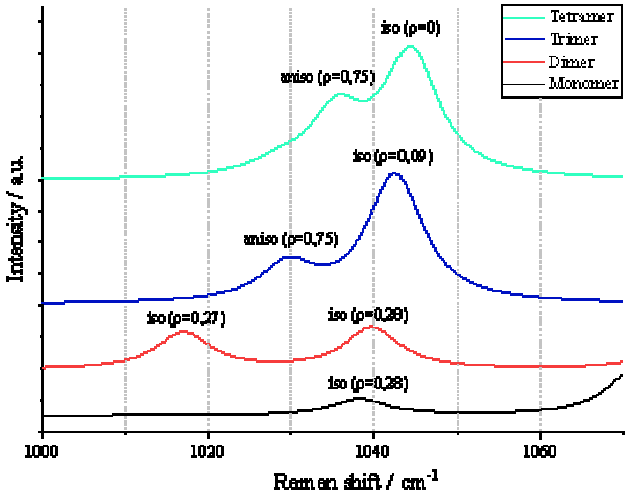

Figure 6. Calculated Raman spectra of methanol clusters in the range of 1000–1070 cm^{-1} (ρ – depolarization ratio).

O-H stretching. Figure 7 shows the calculated Raman spectra of the O-H stretching vibrational bands of methanol clusters without *scale factor*. From the calculated Raman spectrum, we can see that the wave number of the partially symmetric O-H vibrational band is 3850 cm^{-1}. The depolarization ratio of this band is 0.25. The wave numbers of the two O-H bands

formed in the dimer spectrum are 3829 and 3588 cm^{-1}, respectively. The depolarization ratio of these bands is 0.2 and 0.25, respectively. In this case, we can observe that the band of the O-H bond, which forms a mutual hydrogen bond with the oxygen atom of the neighboring molecule, is sharply shifted to a lower wave number. However, both bands are isotropic. Therefore, we can explain that the transition dipole moment is not formed due to the mutual orientation of the molecules in dimer formation. The depolarization ratio of the band at wave number 3591 cm^{-1} in the cyclic trimer spectrum is 0.74. Thus, this spectral band is anisotropic. The depolarization ratio of the band at 3544 cm^{-1} is 0.09. This means that the band is isotropic. Therefore, the difference in wave numbers of the isotropic and anisotropic components in the vibrational spectrum of the cyclic trimer is $\nu_{NCE} = \nu_{anisot} - \nu_{isot}$ =+47 cm^{-1}. Figure 7 shows that three spectral peaks formed in the spectrum of the cyclic tetramer. The spectral band at wave number 3357 cm^{-1} is isotropic (ρ=0.09), while the other two bands at wave numbers 3424 and 3467 cm^{-1} are anisotropic. Both of these anisotropic components have a depolarization ratio of 0.75.

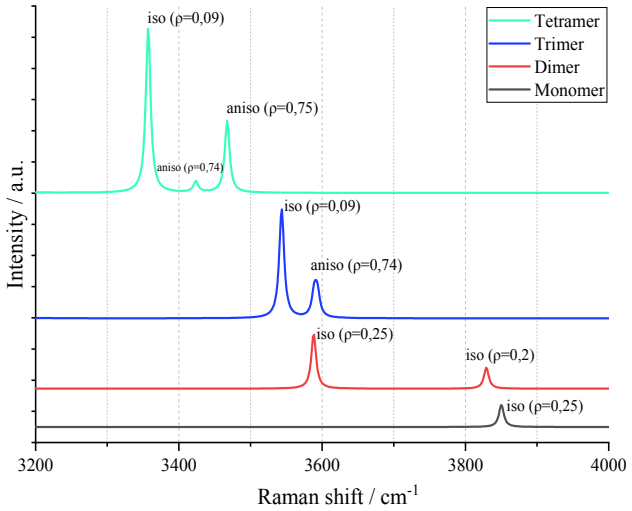

Figure 7. Calculated Raman spectra of O-H stretching of methanol clusters (ρ – depolarization ratio).

If the NCE values for the two anisotropic components are calculated independently, the values are +67 and +110 cm^{-1}, respectively (the experimental value is +75 cm^{-1}). As a result, the spectral bands in 3357 and 3424 cm^{-1} are quite similar to the experiment's wave number and NCE values. The characteristics of the polarized Raman spectrum of the O-H spectral band of the cyclic tetramer, like the C-O, were in agreement with experiments. Because the main cause of NCE generation is the interaction between transition dipoles, in the dipole-dipole orientational analysis, we found that the dipole pair in the tetramer is both orientationally symmetric and has larger intermolecular interaction energy than the dipole pair in the trimer.

IV. Conclusions

In this work, the optimal geometric structure and vibrational spectra of liquid methanol were investigated using the DFT method B3LYP/6–311++G (*d*, *p*) basis set. Quantum-chemical calculations revealed that methanol's dimer cluster cannot form a closed (noncyclic) conformation. As a result, molecules can change their molecular orientation relative to one another, and the potential energy of a dipole-dipole interaction between molecules is zero. This phenomenon was also confirmed by the calculated Raman spectrum. The calculated Raman spectrum indicated that the dimer cluster's C-O and O-H spectral bands do not generate anisotropic components.

The wave numbers of the isotropic and anisotropic components of the cyclic trimer and tetramer clusters were determined based on the calculated Raman spectrum. And based on these results, the value of the noncoincidence was determined. The calculation results showed that the polarized Raman spectrum characteristics of the cyclic tetramer are the most comparable to the experimental data.

Acknowledgments. This work is supported by a project number FZ-20200929385, Ministry of Higher Education, Science and Innovation, Republic of Uzbekistan.

References

[1] P. Mirone, G.J. Fini. Chem. Phys. **71**, No.5, 2241-2243 (1979).
[2] J L. McHale, C.H. Wang. J. Chem. Phys. **73**, No.8, 3600-3606 (1980).
[3] J.L. McHale. J. Chem. Phys. **75**, No.1, 30-35 (1981).
[4] J.L. McHale. J. Chem. Phys. **77**, No.5, 2705-2707 (1982).
[5] C. Perchard, J. Perchard. Chem. Phys. Lett. 27, No.3, 445-447 (1974).
[6] D.E. Logan. Chem. Phys. **103**, No.2-3, 215-225 (1986).
[7] D.E. Logan. Chem. Phys. **131**, 199-207 (1989).
[8] H. Torii, M. Tasumi. J. Chem. Phys. **99**, No.11, 8459-8465 (1993).
[9] H. Torii. J. Chem. Phys. **103**, No.15, 2843-2850 (1999).
[10] E.W. Knapp. J. Chem. Phys. **81**, No.2, 643-652 (1984).
[11] T.W. Zerda, H.D. Thomas, M. Bradley, J. Jonas. J. Chem. Phys. **86**, No.6, 3219-3224 (1987).
[12] R.J. Bartholomew, D.E. Irish. J. Raman Spectrosc. **29**, No.2, 115-122 (1998).
[13] A. Sokolowska. J. Raman Spectrosc. **30**, No.7, 507-509 (1999).

[14] M. Giorgini, H. Torii, M. Musso, and G. Döge. Mol. Phys. **94**, No.5, 821-828 (1998).
[15] M.G. Giorgini, M. Musso, A. Asenbaum, G. Döge. Mol. Phys. **98**, No.12, 783-791 (2000).
[16] M. Giorgini, M. Musso, H. Torii. J. Chem. Phys. **109**, No.26, 5846-5854 (2005).
[17] M. Musso, H. Torii, P. Ottaviani, A. Asenbaum, M.G. Giorgini. J. Chem. Phys. **106**, No.43, 10152-10161 (2002).
[18] G. Döge, D. Schneider, A. Morresi, Mol. Phys. **80**, No.3, 525-531 (1993).
[19] T.G. Devi, K. Kumarю Spectrochimю Acta: A Mol. Biomol. Spectrosc. **62**, No.4-5, 972-979 (2005).
[20] G. Upadhyay, T.G. Devi, R.K. Singh, A. Singh, P.R. Alapati. Spectrochim. Acta: A Mol. Biomol. Spectrosc. **109**, 239-246 (2013).
[21] D.K. Singh, S.K. Srivastava, B.P. Asthana, Chem. Phys. **380**, No.1-3, 24-33 (2011).
[22] F.H. Tukhvatullin, V.E. Pogorelov, A. Jumabaev, H.A. Hushvaktov, A.A. Absanov, A. Shaymanov. J. Mol. Struct. **881**, No.1-3, 52-56 (2008).
[23] H.A. Hushvaktov, F.H. Tukhvatullin, A. Jumabaev, U.N. Tashkenbaev, A.A. Absanov, B.G. Hudoyberdiev, B. Kuylive. J. Mol. Struct. **1131**, 25-29 (2017).
[24] Y. Sun, R. Zheng, Q. Shi. J. Chem. Phys. B **116**, No.15, 4543-4551 (2012).
[25] H. Wang, H. Xu, Q. Liu, X. Zheng. RSC Adv. **10**, 30982-30989 (2020).
[26] Y. Han, R. Liu, C. Jiang, H. Wang, X. Zheng, J. Mol. Liq. **335**, 116224 (2021).
[27] Z. Wang, Y. Han, Q. Peng, C. Jiang, H. Wang. J. Mol. Liq. **387**, 122658 (2023).
[28] R.T. Bailey. Infrared and Raman Studies of Molecular Motion. Molecular Spectroscopy (The Chemical Society) **2**, 173 (1974).
[29] J. Zhang, M. Dolg. Phys. Chem. Chem. Phys. **17**, No.37, 24173-32418 (2015).
[30] M.J. Frisch, G.W. Trucks, H.B. Schlegel, G.E. Scuseria, M.A. Robb, J.R. Cheeseman, G. Scalmani, V. Barone, B. Mennucci, G.A. Petersson, H. Nakatsuji, M. Caricato, X. Li, H.P. Hratchian, A.F. Izmaylov, J. Bloino, G. Zheng, J.L. Sonnenberg, M. Hada, M. Ehara, K. Toyota, R. Fukuda, J. Hasegawa, M. Ishida, T. Nakajima, Y. Honda, O. Kitao, H. Nakai, T. Vreven, J.A. Montgomery, Jr., J.E. Peralta, F. Ogliaro, M. Bearpark, J.J. Heyd, E. Brothers, K.N. Kudin, V.N. Staroverov, R. Kobayashi, J. Normand, K. Raghavachari, A. Rendell, J.C. Burant, S.S. Iyengar, J. To-masi, M. Cossi, N. Rega, J.M. Millam, M. Klene, J.E. Knox, J.B. Cross, V. Bakken, C. Adamo, J. Jaramillo, R. Gomperts, R.E. Stratmann, O. Yazyev, A.J. Austin, R. Cammi, C. Pomelli, J.W. Ochterski, R.L. Martin, K. Morokuma, V.G. Zakrzewski, G.A. Voth, P. Salvador, J.J. Dannenberg, S. Dapprich, A.D. Daniels, Ö. Farkas, J.B. Foresman, J.V. Ortiz, J. Cioslowski, and D.J. Fox. Gaussian 09 (Gaussian, Inc., Wallingford CT, 2009).
[31] R. Dennington, T.A. Keith, J.M. Millam, GaussView. Version 6, Semichem Inc., Shawnee Mission, KS (2016).
[32] A. Jumabaev, U. Holikulov, H. Hushvaktov, A. Absanov, L. Bulavin. Ukr. J. Phys. **67**, No.8, 602 (2022).
[33] R. Ludwig. Chem. Phys. Chem. **6**, No.7, 1369-1375 (2005).
[34] S.L. Boyd, R.J. Boyd. J. Chem. Theory Comput. **3**, No.1, 54-61 (2007).
[35] A. Malloum. J. Conradie, Data Br. **40**, 107818 (2022).
[36] A.S. Kazachenko, U. Holikulov, N. Issaoui, O.M. Al-Dossary, I.S. Ponomarev, A.S. Kazachenko, L.G. Bousiakou. Z. fur Phys. **238**, No.4, 683-705 (2024).
[37] U. Holikulov, A.S. Kazachenko, N. Issaoui, A.S. Kazachenko, M. Raja, O. M. Al-Dossary, Z. Xiang. Spectrochim. Acta: A Mol. Biomol. Spectrosc. **320**, 124600 (2024).
[38] A.S. Kazachenko, N. Issaoui, U. Holikulov, O.M. Al-Dossary, I.S. Ponomarev, A.S. Kazachenko, L.G. Bousiakou. Z. fur Phys. **238**, No.1, 89-114 (2024).
[39] U.A. Holikulo. Uzb. Fiz. J. **25**, No. (2023).
[40] T. Koopmans. Phys. **1**, No.1-6, 104-113 (1934).
[41] V. Tripathi, M.K. Ramanathan. RSC Advances **11**, No.47, 29207-29214 (2021).

Метанолнинг C-O ва O-H тебраниш режимларининг мос тушмалик эффекти: қутбланган Раман ва DFT тадқиқоти

А. Жумабаев[1], Ҳ.А. Хушвақтов[1], Ў.А. Холикулов[1], Ш.Ш. Ёрматов[1], Б.Е. Ниязхонова[2]

[1]Самарқанд давлат университети, Университет хиёбони 15, 140104, Самарқанд, Ўзбекистон
[2]Бухоро давлат университети, М. Иқбол кўчаси 11, 200118, Бухоро, Ўзбекистон

Ушбу тадқиқотда метанолнинг оптимал геометрияси ва тебраниш хусусиятлари қутбланган Раман спектроскопияси ва DFT таҳлил ёрдамида ўрганилди. Метанол молекуляр кластерларининг глобал минимум структуралари ABCluster дастури ёрдамида ҳосил қилинди. DFT ва FMO таҳлиллар турли метанол молекуляр кластерларини структуравий ва термодинамик жиҳатдан текшириш учун қўлланилди. Ушбу усуллардан фойдаланиб, метанол димер, тример ва тетрамер кластерларининг молекулалараро ўзаро таъсир потенциал энергиялари ва HOMO-LUMO энергия бўшлиқлари ҳисоблаб чиқилган. Натижада, метанолнинг структуравий ва термодинамик барқарорлиги энг юқори бўлган димер-helical, циклик тример-uud ва циклик тетрамер-udud кластерлари аниқланди. Метанол C-O ва O-H спектрал диапазонларининг изотроп ва анизотроп ташкил этувчиларини аниқлаш учун экспериментал ва ҳисоблаш усуллари қўлланилди. Олинган маълумотлар шуни кўрсатдики, димер кластерида анизотроп ташкил этувчи ҳосил бўлолмайди. Циклик тетрамер кластерининг қутбланган Раман спектрининг характеристикалари экспериментал натижаларга яқин эканлиги аниқланди.

Калит сўзлар: DFT, FMO, ABCluster, изотроп, анизотроп, Раман мос тушмаслик эффекти.